

# Influence of Discharge Oscillation on Hall Thruster Performance\*

Naoji Yamamoto, Takafumi Nakagawa, Kimiya Komurasaki and Yoshihiro Arakawa  
 Department of Aeronautics and Astronautics, University of Tokyo  
 Hongo 7-3-1, Bunkyo-ku, Tokyo, 113-8656, Japan  
 +81-3-5841-6586  
[naoji@al.t.u-tokyo.ac.jp](mailto:naoji@al.t.u-tokyo.ac.jp)

IEPC-01-055

**Influence of discharge oscillations at frequency range of 10-100kHz was investigated using the 1kW class sheath type Hall thruster. Lifetime, that is, wall erosion was examined by means of spectroscopy. The erosion rate in unstable operation was twice as large as that in stable operation. Plume divergence was also measured. The full angle at half maximum of thruster plume was increased from 14.4 to 18.2 degree when the operation was changed from stable operation to unstable operation. However, the oscillation amplitude had little relation with the erosion rate, the plume divergence and the thruster performance. These results would indicate that the ionization zone configuration would affect lifetime, the plume divergence, thruster performance and oscillation rather than oscillation in itself would affect lifetime, the plume divergence and thruster performance.**

## Nomenclature

## Subscripts

$A$	: oscillation amplitude
$A_{ki}$	: transition probability from state k to i
$B$	: magnetic flux density
$D$	: diffusion coefficient
$E_i$	: energy of state i
$g_i$	: degeneracy of state i
$I$	: current
$I_d$	: discharge current
$I_{sp}$	: specific impulse
$k_B$	: Boltzmann's constant
$L$	: ionization zone length
$\dot{m}$	: mass flow rate
$M$	: mass
$N$	: number density
$r_L$	: Larmor radius
$T$	: temperature
$V$	: velocity
$V_d$	: discharge voltage
$w$	: chamber width
$Y$	: sputter yield
$\gamma$	: ionization coefficient
$\tau$	: measurement time
$\nu$	: collision frequency
$\sigma$	: collision cross section

$e$	: electron
erosion	: erosion material
$i$	: ion
$n$	: neutral atom
$w$	: wall
$0$	: anode
$1$	: exit

## Introduction

A Hall thruster is one of the promising thrusters for satellite station keeping and orbit transfer, since it delivers the specific impulse of 1000 – 3000sec and the thrust efficiency is more than 50%. Ion beam density of Hall thrusters can be higher than that of ion thrusters because of the existence of electrons in the ion acceleration zone.

They are categorized into two types: linear type and sheath type. One of the linear type Hall thrusters is “Stationary Plasma Thruster” (SPT), which has been developed in Russia. The acceleration channel length is longer than the channel width and the channel walls are made of ceramics. And, “Thruster with Anode Layer”(TAL), having been developed in Russia as well, is categorized into sheath type. It has a short discharge

chamber. Guard rings, which protect magnetic pole pieces, were made of electric conductor, being kept at the cathode potential. Owing to this design, the lifetime of sheath type is considered longer than that of linear type. However, it can work in a very limited range of operational condition compared with the linear type.

One of the problems in Hall thrusters is discharge current oscillation, especially at frequency range of 10-100kHz, which might affect the performance and lifetime of the thruster. In our previous research, the discharge suddenly ceased due to this oscillation [1]. Although there are many studies in this range oscillation [2]-[5], the relation between oscillation and performance or lifetime has not investigated. The aim of this study is to investigate the relation between oscillation and thruster performance such as  $I_{sp}$ , plume divergence, lifetime.

## Experimental Equipment

### Thrusters

Figure 1 shows the cross-section of laboratory-made 1kW class sheath type Hall thruster. It has two guard rings made of stainless steel. The inner and outer diameter of the discharge chamber are 48mm and 62mm, respectively. The outer diameter of discharge chamber can be changed to 72mm. The anode is located at 3mm upstream end of the chamber. The solenoidal coil is set at the center of the thruster to apply radial magnetic fields in the chamber. Magnetic flux density is maximum at the chamber exit and minimum at the anode.

Xenon was used as a propellant gas. As an electron source, a hollow cathode (Ion tech product 7HCN-001-001) was used in almost all cases. Cathode flow rate was fixed at 0.27 mg/s. A filament cathode ( $\phi$  0.27mm $\times$ 500mmL $\times$ 3, 20V $\times$ 20A) was used when oscillation characteristics were measured, since the hollow cathode in itself can be a noise source [1][6].

### Emission spectroscopic measurement

Figure 2 shows a schematic of optical measurement system. A focusing point was set at 5mm downstream of the thruster exit with a 500mm focal length collimating lens. The focusing point size is 1 mm. A spectrometer (Hamamatsu Photonics product PMA-50) was used. The spectrometer grating was 1200 grooves/mm and the dispersion was 0.04nm/ch. The wavelength resolution was 0.09nm.

### Ion collector

Figure 3 shows a schematic of ion collector. Ion collector has three grids in order to avoid the influence of Charge Exchanged ions; one is floating grid, another is electron-retarding grid, and the other is ion-retarding grid. This collector was set at 500mm downstream of the thruster and rotated from  $-90$  to  $90$  degree.

### Vacuum Chamber

Experiments were performed in two space chambers. One is a 0.8m diameter by 2.5m long vacuum chamber. Pumping speed is 12000l/s and the ultimate base pressure is  $1.3 \times 10^{-3}$  Pa. The operation pressure is less than  $3.6 \times 10^{-2}$  Pa. The other is a 2m diameter by 3m long vacuum chamber. Pumping speed is 30000l/s and the ultimate base pressure is  $4.5 \times 10^{-4}$  Pa. The operation pressure is less than  $5.3 \times 10^{-3}$  Pa.

Spectroscopic measurements were done in the small chamber because of the restriction of the facility. The other experiments were done in the large chamber.

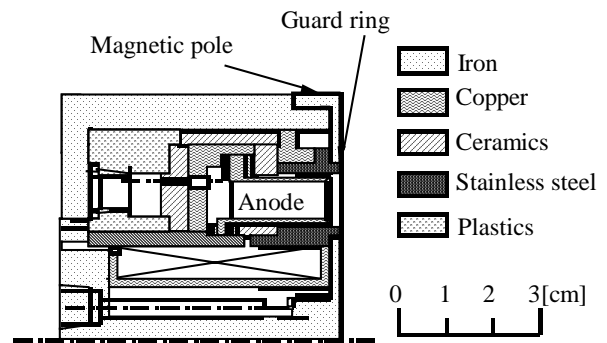


Fig. 1 Cross section of sheath type Hall thruster

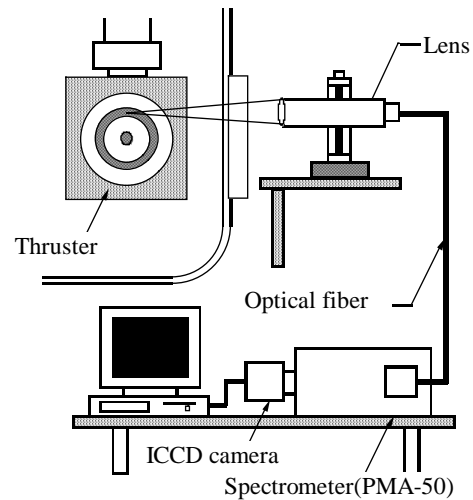


Fig. 2 Schematic of optical measurement system

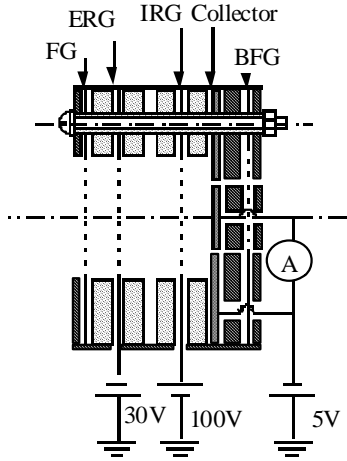


Fig.3 Schematic of ion collector

### Oscillation Characteristics

Before discussing the influence of oscillation on thruster performance and the erosion rate, oscillation characteristics are described. The detail is shown in our previous research [5].

The amplitude of oscillation is defined as

$$A = \frac{R.M.S}{\bar{I}_d} = \frac{1}{\bar{I}_d} \sqrt{\frac{\int_0^\tau (I_d - \bar{I}_d)^2}{\tau}}, \quad (\bar{I}_d = \frac{\int_0^\tau I_d}{\tau}) \quad (1)$$

Figure 4 shows the oscillation characteristics versus magnetic flux density. The oscillation characteristics are changed sensitively with magnetic flux density and can be categorized into three regimes. The feature of each regime was shown below.

Figure 5 (a) shows the discharge current trace in Regime 1. Though the oscillation amplitude was large, operation was stable in this regime. This was seen at low magnetic flux density. Figure 5 (b) shows the discharge current trace in Regime 2. In Regime 2, the oscillation amplitude was less than 0.05 and the discharge was stable. In Regime 1 and Regime 2, the electron current was proportional to  $B^2$ . Hence, electrons are thought to move to the anode with classical diffusion. Figure 5 (c) shows the discharge current trace in Regime 3. The oscillation in Regime 3 was the strongest oscillation among the all. The oscillation amplitude was increased with magnetic flux density. The discharge suddenly ceased beyond the critical magnetic flux density. The electron current

wasn't proportional to  $B^2$  but was almost constant with magnetic flux density.

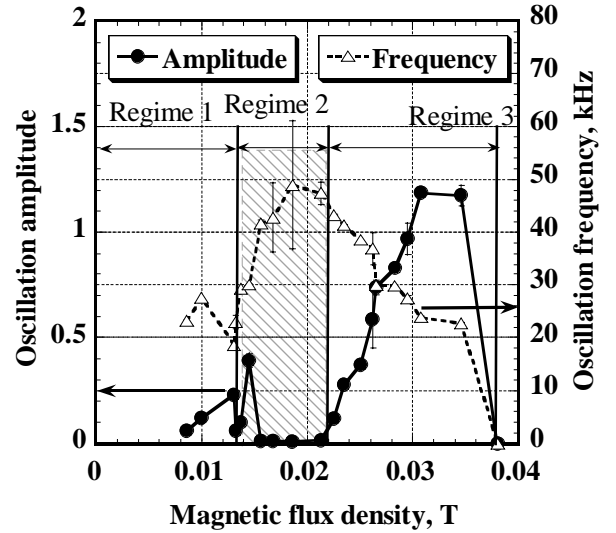
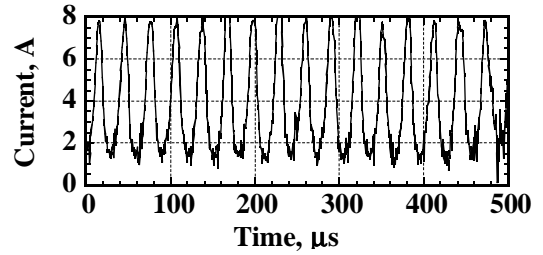
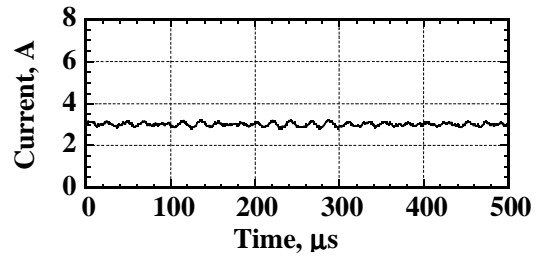


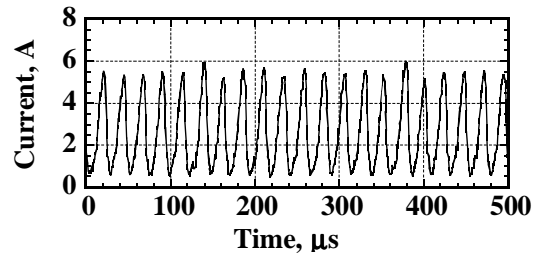
Fig. 4 Oscillation characteristics at  $\dot{m} = 2.04 \text{ mg/s}$ ,  $V_d = 250 \text{ V}$ ,  $w = 7 \text{ mm}$



(a)



(b)



(c)

Fig.5 Discharge current trace

(a) Regime 1, (b) Regime 2, (c) Regime 3

## Results and Discussion

### Lifetime

The influence of oscillation on the lifetime was investigated. The lifetime would be limited by the erosion of the chamber wall. The wall erosion was examined by means of emission spectroscopy of the plume, instead of long-term lifetime test. The intensity of erosion material spectra can be a good indicator of an erosion rate. The intensity of the light emitted with transition is proportional to the population of the excited state, the population is a function of neutral atom number density of erosion material, electron density and electron temperature. The electron number density and the electron temperature in the measurement position were almost constant through this experiment. Thus, the intensity has a strong correlation with the erosion rate. The guard rings were made of copper instead of stainless steel in order to sense the difference in the erosion rate easily in various operational conditions. Though the anode was also made of copper, it can't affect the result. The transition data of this measurement was shown in Table 1 quoted from NIST database [7].

Figure 6 shows the relation between the intensity of Cu I transition at 510.55nm and magnetic flux density. The difference of oscillation characteristics in Fig. 4 and Fig. 6 might be derived from the distinction of cathode. The tendency of other lines was almost the same. The intensity in Regime 2 was smaller than that in Regime 1 or Regime 3. However, there is little relation between the erosion rate and the oscillation amplitude. In addition, the erosion rate was decreased with magnetic flux density and an increase of magnetic flux density was more effective in the decrement of the erosion rate than the suppression of oscillation.

**Table 1.** Transition data of Cu I

Wave length, nm	$E_{k\gamma}$ , eV	$A_{ki}$ $10^{-8}$ -s	$g_i - g_k$
402.263	6.87	0.190	2 - 4
406.264	6.87	0.210	4 - 6
465.112	7.74	0.380	10 - 8
510.554	3.82	0.020	6 - 4
515.324	6.19	0.600	2 - 4
521.82	6.19	0.750	4 - 6
570.024	3.82	0.002	4 - 4
578.213	3.79	0.017	4 - 2

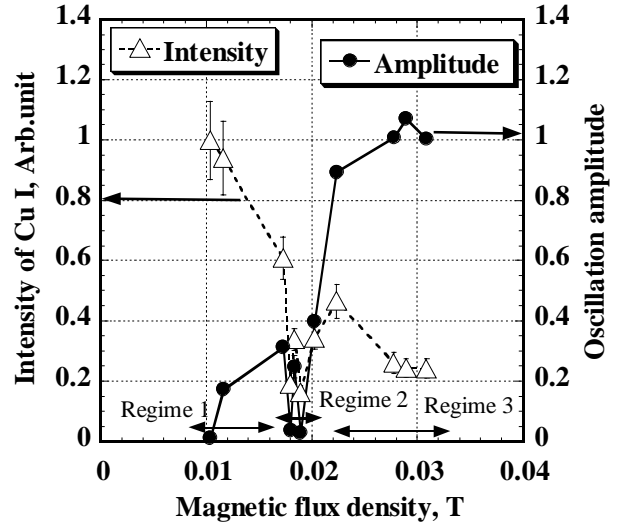


Fig.6 Emission intensity of Cu I at  $\dot{m}=2.04\text{mg/s}$ ,  
 $V_d=250\text{V}$ ,  $w=7\text{mm}$

To investigate the cause of this characteristics of the erosion rate, the current density is need to be measured, since the erosion rate is written as,

$$\dot{N}_{erosion} = \frac{I_w Y}{e} \quad (2)$$

Thus, the ion current into the guard rings was estimated. The guard rings were kept at cathode potential, only ion would collide with the guard rings. Thus, the ion current would be estimated as the current into the guard rings. As shown in Fig.7, the ion current into the guard rings in Regime 2 was lower than that in Regime 1 or Regime 3 as well as the erosion rate was. On the other hand, the ion current in large oscillation condition was almost constant despite that the erosion rate was decreased with magnetic flux density, though each of the oscillation amplitude was different. In addition, there was little relation between the ion current and magnetic flux density. It seems that the ion current into the guard rings depended on that oscillation occur or not.

According to Eq. (2) and two facts that the ion current was almost constant with magnetic flux density and that the erosion rate decreased with magnetic flux density, the energy of colliding ion would decrease with magnetic flux density, since a sputter yield depends on ion energy. The energy of ions could be estimated as the plasma potential in ionization zone. Then the plasma potential was measured by an emissive probe.

The emissive probe was made of a 0.1mm in diameter 0.1%thoriated tungsten. Figure 8 shows the axial profile of the plasma potential at the middle of the guard rings. The origin in this figure was the thruster exit. The plasma potential was decreased with magnetic flux density. Hence, the erosion rate decreased with magnetic flux density despite the ion current was almost constant. However, the decrease in erosion rate in Regime 2 would be due to the decrease in the ion current into guard rings.

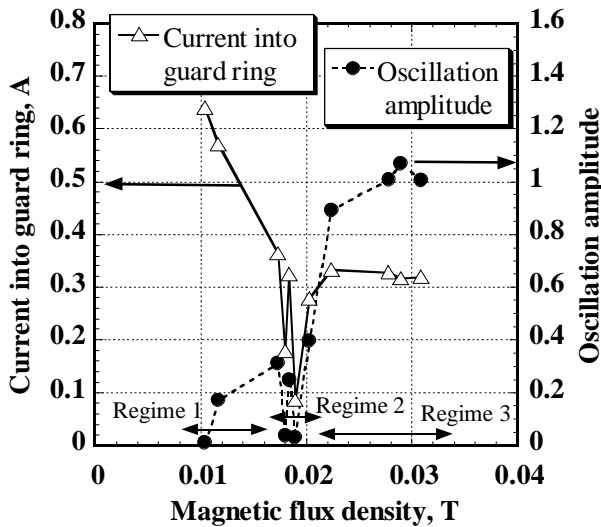


Fig.7 Current to guard ring at  $\dot{m}=2.04\text{mg/s}$ ,  $V_d=250\text{V}$ ,  $w=7\text{mm}$

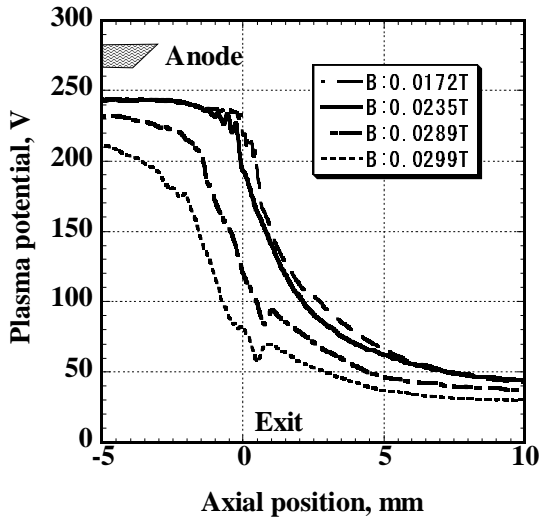


Fig.8 Axial profile of plasma potential at  $\dot{m}=4.08\text{mg/s}$ ,  $V_d=250\text{V}$ ,  $w=12\text{mm}$

### Plume divergence

Figure 9 shows the relation between the full angle at half maximum and magnetic flux density. There was little relation between the oscillation amplitude and the plume divergence except that the minimum point of the plume divergence was same as the minimum point of the oscillation amplitude.

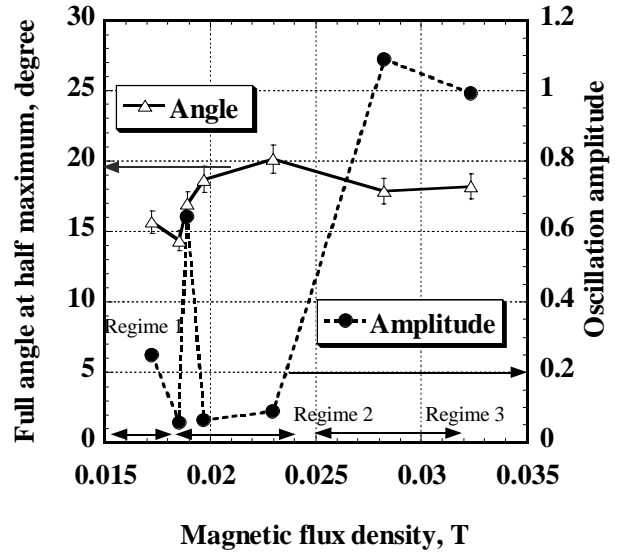


Fig.9 Relation between the full angle of half maximum and magnetic flux density at  $\dot{m}=4.08\text{mg/s}$ ,  $V_d=250\text{V}$ ,  $w=12\text{mm}$

### Thruster performance

Figure 10 shows  $I_{sp}$  versus magnetic flux density.  $I_{sp}$  decreased with magnetic flux density and there was little relation between the oscillation amplitude and  $I_{sp}$ , since the propellant utilization decreased with magnetic flux density as shown in Fig. 11 and beam energy efficiency was decreased with magnetic flux density.

Figure 12 shows thrust efficiency versus magnetic flux density. The efficiency had little relation with oscillation as well as  $I_{sp}$ . Though the thrust was decreased with magnetic flux density, the discharge current was also decreased with magnetic flux density until Regime 3. Thus, there is the most efficient operational condition, and almost all case it is in Regime 2.

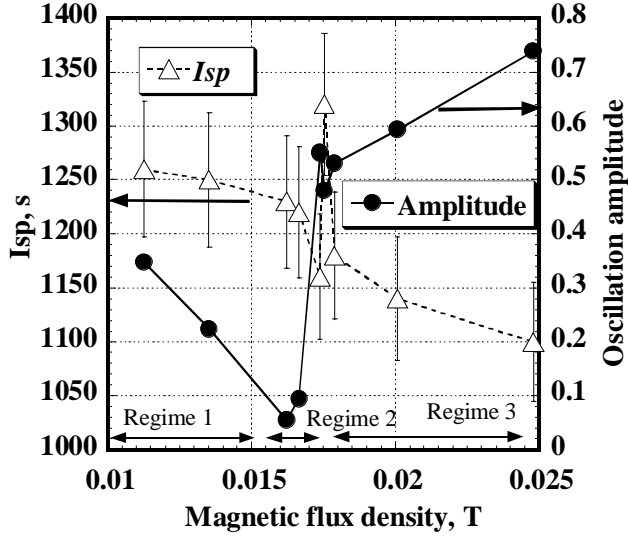


Fig.10 Specific impulse versus magnetic flux density at  $\dot{m}=2.72\text{mg/s}$ ,  $V_d=250\text{V}$ ,  $w=12\text{mm}$

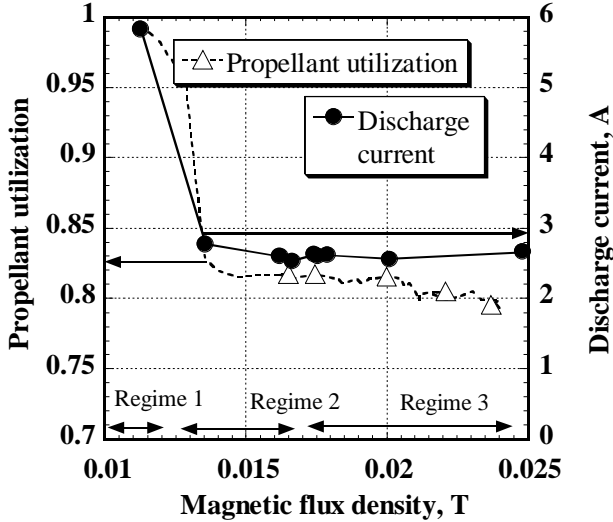


Fig.11 Propellant utilization versus magnetic flux density at  $\dot{m}=2.72\text{mg/s}$ ,  $V_d=250\text{V}$ ,  $w=12\text{mm}$

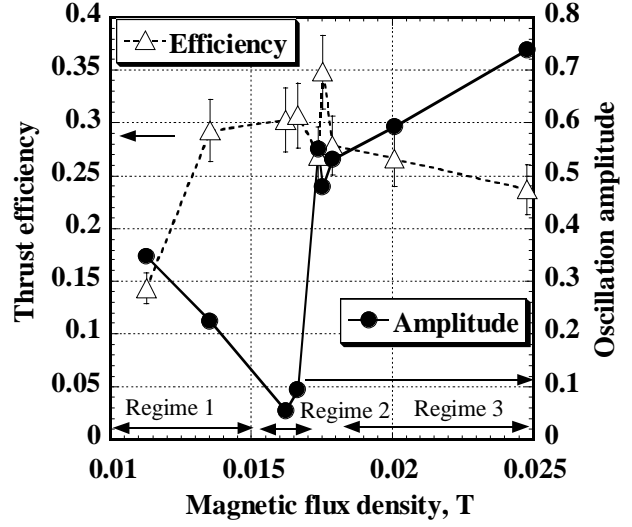


Fig.12 Thrust efficiency versus magnetic flux density at  $\dot{m}=2.72\text{mg/s}$ ,  $V_d=250\text{V}$ ,  $w=12\text{mm}$

These above the results might indicate that the oscillation in itself might have little effect on the erosion rate, the plume divergence and the thruster performance. It might be reasonable that oscillation wouldn't cause electric field distortion and that change in ionization zone configuration would lead to an oscillation regime changing and would affect the erosion rate or the plume divergence. As magnetic flux density increases, the ionization zone configuration is thought to change as shown in Fig. 13. Ionization zone length  $L$  would be decreased with magnetic flux density and the end of the ionization zone would move to anode.

According to our previous study [5], the instability condition of ionization oscillation is written as,

$$(-2.718 \frac{N_{n1}}{N_{n0} + N_{n1}} + 1)(\gamma N_n + \frac{V_{e1} - V_{e0}}{L}) - \gamma N_e < 0 \quad (3)$$

Considering that electron would move to anode with classical diffusion, electron velocity  $V_e$  is written as,

$$V_e = - \frac{M_e N_n < \sigma v >_{en}}{e B^2} (E + \frac{k_B T_e}{e} \frac{\nabla N_e}{N_e}) \quad (4)$$

Ionization length  $L$  would be estimated as,

$$L = \alpha r_{lc} = \frac{\alpha}{B} \sqrt{\frac{8 m_e k_B T_e}{\pi e}} \quad (\alpha: 2-3) \quad (5)$$

In addition, electron temperature may be estimated as.

$$T_e = 0.013 \frac{V}{\sqrt{B}} \quad (6)$$

Thus, the left side of inequality (3) would be rewritten as,

$$\begin{aligned} \frac{V_{e1}-V_{e0}}{L} &\propto \frac{\frac{\alpha_0}{B^{2.5}}(E_0 + \alpha_1 \frac{T_e}{L}) - \frac{\beta_0}{(B + \Delta B)^{2.5}}(E_0 + \beta_1 \frac{T_e}{L})}{\frac{\chi}{B}} \\ &= \frac{\alpha_2}{B^{1.5}} \left\{ (1 + \alpha_3 \sqrt{B}) - \beta_2 (1 + \beta_3 \sqrt{B}) \left( 1 - 2.5 \frac{\Delta B}{B} \right) \right\} \\ &= \frac{\alpha_2}{B^{1.5}} \left\{ (1 + \alpha_3 \sqrt{B}) - \beta_2 (1 + \beta_3 \sqrt{B}) (1 - 2.5 \kappa L) \right\} \\ &= \frac{\alpha_2}{B} \left\{ \alpha_4 \sqrt{B} + \alpha_5 B + \beta_4 + \beta_5 \frac{1}{\sqrt{B}} \right\} \end{aligned} \quad (7)$$

$\alpha_i, \beta_i, \chi, \kappa$ : Constant

Thus, the left side of Eq. (3) would change from negative to positive and then negative when magnetic flux density was increased as shown in Fig.14.

According to oscillation theory of Baronov [2][8], the instability condition of ionization oscillation is written as,

$$\left( \frac{\partial D_e}{\partial x} - V_n \right)^2 > \frac{(N_n - N_e)^2}{N_n} D_e \gamma \quad (8)$$

Inequality (8) is rewritten as,

$$\begin{cases} \frac{\partial D_e}{\partial x} < Const \text{ or } B^2 > \{V_d (Const - V_d^{-3})\}^{-1} (B_a < B < B_b) \\ V_n - \frac{\partial D_e}{\partial x} < Const \text{ or } \frac{V_d}{B^\nu} > Const \quad (B > B_c) \end{cases}$$

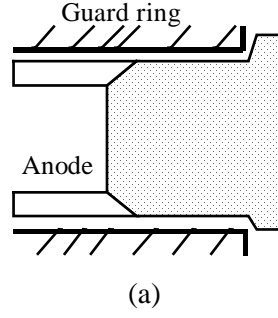
( $1 < \nu < 1.5$ )

(9)

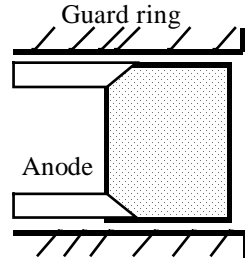
The predicted stable operation condition of Eq. (9) would be similar to that of Eq. (3). That is, predicted stable operating condition would agree with experimental results.

Now considering the plume divergence. In the configuration of (a) and (c), electric field in the ionization zone would be more distorted than that in (b). Thus the plume divergence would be minimum in (b).

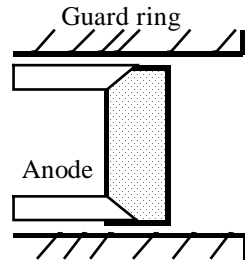
In like wise, the distorted electric field would make ion current into guard rings enlarge. Thus erosion rate would be the smallest of all in the configuration as Shown in (b).



(a)



(b)



(c)


 ionization zone

Fig. 13 Scheme of ionization zone configuration, (a) low magnetic flux density (b) middle magnetic flux density (c) high magnetic flux density

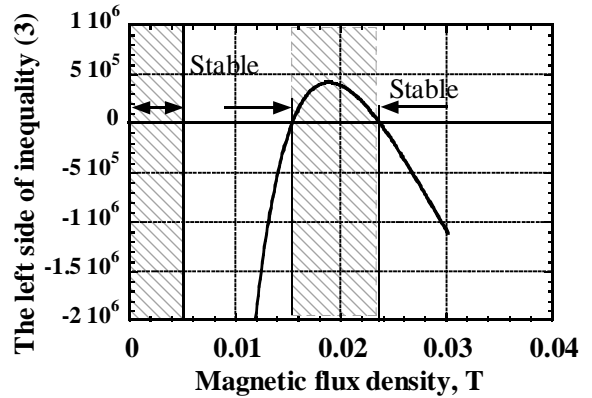


Fig.14 The left side of inequality (3) versus magnetic flux density

## Conclusion

The influence of discharge oscillation on the performance and the lifetime of Hall thrusters was investigated.

- The erosion rate in regime 3 was twice as large as that in Regime 2. However, the relation between the erosion rate and magnetic flux density was stronger than one between the erosion rate and the oscillation. One of the reasons of this was the decrement of the ion energy with magnetic flux density decreasing.
- The full angle at half maximum of the thruster plume increased from 14.4 to 20.1 degree with oscillation in the same regime. However, the plume divergence decreases with the oscillation amplitude increasing in the same regime.
- $I_{sp}$  decreased with magnetic flux density and there is little relation between  $I_{sp}$  and the oscillation amplitude. The thruster performance has a maximum point and it often appeared in Regime 2. It would depend on the balance of thrust and discharge current.

It might be reasonable that change in ionization zone configuration would cause oscillation regime to change and would affect the erosion rate, the plume divergence and thruster performance.

## References

- [1] Nomura K., Kakimoto H., Komurasaki K., Arakawa Y, "Acceleration Channel Length and Discharge Instability of Hall Thruster" The 42nd Space Sciences and Technology Conference, 1D4,1998 (in Japanese)
- [2] Baronov V. I., Nazarenko Yu. S., Petrosov V. A., Vasin A. I., and Yashonov Yu. M. "Theory of oscillations and Conductivity For Hall Thruster" AIAA 96-3192, 32nd AIAA/ASME/SAE/ASEE joint Propulsion Conference. July 1996, Lake Buena Vista, FL
- [3] Fife, J. M., Martinez-Sanchez, Manuel, and Azabo, James "A numerical study of low-frequency discharge oscillations in Hall thrusters" AIAA96-3052, 33rd AIAA/ASME/SAE/ASEE joint Propulsion Conference. July Seattle, WA, July, 1997
- [4] Darnon F., Kadlec-Philippe C., Bouchoule A., and Lyszuk M. "Dynamic Plasma & Plume Behavior of SPT thrusters" AIAA98-3644, 34th AIAA/ASME/SAE/ASEE joint Propulsion Conference. July 1998, Cleveland, OH
- [5] Yamamoto N., Nakagawa T., Komurasaki K. and Arakawa Y. "Observation of plasma Fluctuations in Hall Accelerators" Advances in Applied Plasma Science Vol. 3, 2001;pp95-100
- [6] Nishiyama K., Shimizu Y., Funaki I., Kuninaka H. and Toki K."Electromagnetic Noise from a Microwave Discharge Neutralizer and Hollow Cathode" Japan Soc. Aero. Space Sci. 49, 2000, pp84-91 (in Japanese)
- [7]<http://www.physics.nist.gov>
- [8] Baronov V. I., Nazarenko Yu. S., Petrosov V. A., Vasin A. I., and Yashonov Yu. M. "The Ionization Oscillations Mechanism in ACD" IEPC95-059, 24th International Electric Propulsion Conference. Moscow, Russia, September 1995



